



Physical modelling of the stability of a revetment breakwater built on reclaimed coral calcareous sand foundation in the South China sea—random waves and dense foundation

Yu Zhang^{a,b}, Jianhong Ye^{a,*}

^a State Key Laboratory of Geomechanics and Geotechnical Engineering, Institute of Rock and Soil Mechanics, Chinese Academy of Sciences, Wuhan, 430071, China

^b University of Chinese Academy of Sciences, Beijing, 100049, China

ARTICLE INFO

Keywords:

Random waves
JONSWAP spectrum
Physical model test in wave flume
Revetment breakwater in the SCS
Dense foundation
Calcareous coral sand foundation

ABSTRACT

In the past several years, China has successfully constructed and enlarged several lands on the top of some coral reefs in the South China Sea (SCS thereafter) by the way of reclamation. A great number of revetment breakwaters have been built at the margins of these reclaimed coral reef islands, to defend these artificial lands from scouring and intensive wave impact. In order to quantitatively explore the dynamics characteristics, as well as the stability of these revetment breakwaters and their foundation under extreme wave impact, in this study, five large-scale wave flume physical model tests are conducted adopting a geometric similarity ratio of 1:10, to experimentally investigate the wave impact, displacement of the revetment breakwater, wave overtopping and the pore pressure in the dense calcareous sand foundation under the attack of random waves. Finally, the overall stability of the revetment breakwater is evaluated. The experimental results indicate that the maximum impact on the revetment breakwater applied by the fortified extreme waves reaches up to 6 kPa, the responding pore pressure in the dense coral sand foundation is not very significant, and the maximum volume of wave overtopping can be up to 0.39 m³/h per meter when there is no accropode installed to dissipate wave energy. There is no obvious deformation occurring in the dense foundation, and the displacement of the revetment breakwater is also not significant after long-term wave impacting. Combining all these experimental results, it is concluded that the revetment breakwater can stay stable under the condition of the fortified extreme ocean wave. However, the amount of wave overtopping is considerable, which would result in the delay of the process of the groundwater desalination in these reclaimed islands in the SCS. The test results further indicate that the usage of accropodes can considerably reduce the wave impact and the amount of wave overtopping.

1. Introduction

The South China Sea (SCS) is a vital channel for economic trade and energy transportation in the world, and it contains rich marine oil and gas mineral resources. In the past several years, China has constructed or enlarged several artificial islands on the top of natural coral reefs by the way of reclamation. However, compared with land environment, the marine environment is more severe due to the frequent tropical storms and typhoons occurring in the SCS. A great number of revetment breakwaters have been built along the margin of these reclaimed lands to resist the scouring and impacting caused by extreme waves. As a kind of important coastal protective structure, breakwaters can effectively block the wave impact and wave overtopping, enhance the stability of

the reclaimed reef islands, and reduce the deformation of structure foundation. However, extreme ocean waves would destroy the infrastructures such as breakwaters frequently (Zhang and Ge, 1996). Therefore, it is necessary to study the stability of the revetment breakwater and its foundation under the attack of extreme waves, and it is of great importance to ensure the normal service capabilities of the reclaimed reef islands in the SCS.

Generally, there are two kinds of methods to study the dynamic response, as well as the stability of breakwater and its seabed foundation under wave loading (wave-seabed-structures interaction). They are numerical computation and physical model test, respectively. Previous studies mainly focused on the wave-seabed interaction based on the Biot's consolidation theory (Biot, 1941), including the analytical

* Corresponding author.

E-mail addresses: Jhye@whrsm.ac.cn, Yejianhongcas@gmail.com (J. Ye).

<https://doi.org/10.1016/j.oceaneng.2020.108384>

Received 17 May 2020; Received in revised form 5 November 2020; Accepted 8 November 2020

Available online 25 November 2020

0029-8018/© 2020 Elsevier Ltd. All rights reserved.

solutions (Yamamoto, 1978; Madsen, 1978; Hsu and Jeng, 1994), and finite element modelling (Gatmiri, 1990; Wang et al., 2015). With the development of numerical modelling technique, the mathematical models on wave-seabed-structures interaction were gradually developed and refined. Jeng (2001) proposed a 2D uncoupled finite element method to study the dynamics of soil around a breakwater. Mizutani et al. (1998) and Mostafa et al. (1999) developed a BEM-FEM combined model for the problem of wave-seabed-structures interaction, which was verified by several wave flume tests. In the past decade, several numerical models have been developed to explore the dynamics of marine structures and their seabed foundation under ocean waves or seismic loading (Ye and Wang, 2015), for example, Ye et al. (2013a, 2013b), Ye et al. (2014) developed a coupled/integrated numerical model FSSI-CAS 2D and its 3D version for the fluid-seabed-structures interaction (FSSI) problem. The effectiveness, adaptability and accuracy of the coupled model have been verified by a series of experimental data and several analytical solutions.

For some important large-scale marine engineering, such as breakwater, submarine pipeline, offshore drilling platform, wave flume model tests are frequently conducted to simulate the process of wave-seabed-structures interaction for the following three purposes: (1) Investigating the characteristics of pore pressure responses in seabed foundation under the attack of waves (Demars and Vanover, 1985; Zen and Yamazaki, 1990; Tzang, 1992; Wang et al., 2007), and revealing the seabed liquefaction behavior (Sumer et al., 2006; Kirca et al., 2013); (2) Exploring the wave impact on structures and the wave overtopping without considering seabed foundation, which actually belongs to the field of CFD, e.g., Ju (2004) systematically studied the wave impact force and wave overtopping of a typical chest wall by flume tests; (3) Investigating the complicated interaction between wave, seabed and marine structures. Some typical wave flume physical model tests have been performed in the past (Mizutani et al., 1998; Mostafa et al., 1999; Lu, 2005; Ye et al., 2019). Recently, Yan et al. (2018) analyzed the dynamics characteristics of a semi-cylindrical breakwater and its silty clay foundation under wave impact using an extremely large-scale wave flume device. In recent years, some new revetments have been developed for coastal protection, for example, the articulated concrete block mattress (ACB Mats) revetment. Yamini et al. (2017, 2018) investigated the effect of various parameters on the stability of ACB Mats revetment, and explored the characteristics of wave run-up and run-down by performing laboratory wave flume tests. However, it is worthy to notice that the waves generated in flumes for FSSI problem are mostly regular waves in previous works. According to the irregular characteristics of real ocean waves, random waves that are much closer to real ocean waves, can more effectively simulate the impacting of ocean waves. Of course, there still are some typical wave flume tests in which random waves are involved in literature. They mainly focus on the measurement of the wave overtopping under the attack of random waves (Aminti et al., 1989), the impact pressure of random waves on breakwaters (Galland, 1995; Chen et al., 2019), and the distribution of pore pressure in sandy foundation under the action of regular waves and random waves (Bie et al., 1997). However, to the authors' best knowledge, large-scale wave flume physical model tests never have been conducted to investigate the dynamic response, as well as the stability of the revetment breakwater and its calcareous coral sand foundation built on the reclaimed reef islands under severe random wave impact in the SCS.

The marine environmental loading in the SCS is relatively harsh. According to the official statistics, there are generally 2–3 catastrophic typhoons and 5–6 tropical storms with different intensity occurring in the SCS each year. Generally, the active time of typhoons and tropical storms is about 240 h each year. It could bring obvious disastrous effect to the marine structures in the SCS, for example, the maximum wind speed near to the typhoon center can reach 75 m/s when the super typhoon 'Haiyan' crossed the SCS in 2013, resulting in the damage of a great number of breakwaters in ports and causing huge loss of life and property. The stability of the revetment breakwaters in the SCS also will

Table 1
Similarity ratio of physical quantities in the wave flume tests.

Physical Quantity	Symbol	Similarity Relation	Similarity Ratio
Length	L	λ_L	1:10
Depth	D	$\lambda_D = \lambda_L$	1:10
Height	H	$\lambda_H = \lambda_L$	1:10
Time	t	$\lambda_t = \lambda_L^{1/2}$	$1:\sqrt{10}$
Velocity	V	$\lambda_V = \lambda_L^{1/2}$	$1:\sqrt{10}$
Pressure	p	$\lambda_p = \lambda_L$	1:10
Volume	Q	$\lambda_Q = \lambda_L^2$	1:100

be affected by these catastrophic typhoons and tropical storms in their designed normal performance period. Taking the reclamation project of coral reef islands in the SCS as the engineering background, this study is to investigate the dynamic response and the stability of the revetment breakwater and its calcareous sand foundation under the action of extreme random waves by performing five large-scale wave flume physical model tests. So far as we know, the experimental work presented in this study considering the interaction between the revetment breakwater and its coral sand foundation actually is conducted for the first time in the field of offshore geotechnics for the reclamation project in the SCS. The experimental results presented in this study could provide a scientific basis for the design, construction, and maintenance of the revetment breakwater in the SCS in the future.

2. Experimental setup

2.1. Equipment and similarity ratio

The dimension of the wave flume is 47.0 m (length) \times 1.0 m (width) \times 1.3 m (height). The left side of the flume is equipped with a paddle wave maker (1.0 m \times 1.0 m) controlled by a servo motor, which can generate various waves such as regular waves, random waves, solitary wave, etc. A slope with a length of 7 m and an inclined angle 20° is built at another end of the flume for wave absorption. The physical model is designed according to the real terrain and the size of the revetment breakwater around the reclaimed lands in the SCS. The geometric scale is set as 1:10 according to Froude similarity principle. The similarity relation of physical quantities in the tests is listed in Table 1.

2.2. Physical model and sensors

The schematic map of the physical model designed in this study is shown in Fig. 1. The effective length of the flume is 45.05 m, including the wave propagation section, the physical model zone and the wave absorption section with a length of 30 m, 8.05 m and 7 m, respectively. The physical model includes the revetment breakwater and its foundation. The physical model is installed by two ways: full section or semi-section, as that illustrated in Fig. 2. In wave flume tests, the way of full section is widely adopted, but its disadvantage is that incident waves are blocked by the physical model, resulting in a considerable wave reflection. However, the energy of the reflected waves is difficult to be dissipated, which is unfavorable in flume tests. The reflected waves and incident waves will continuously interact during testing, and further affect the test results. The way of semi-section will significantly reduce the blocking effect and dissipate the energy of reflected waves.

The revetment breakwater is composed of a vertical caisson wall and a S-shaped revetment, which is constructed with concrete. The foundation of the breakwater consists of three kinds of materials: gravels, sand-stones mixture, and calcareous sand. The area of gravels is a triangle with a length of 5.4 m, a height of 0.45 m, and a sloping of 1:12. This area is to simulate the coral reef flat in front of the breakwater. Some rubble mounds with an average diameter of 10 cm are stacked within a range of 1–2 m in front of the breakwater and on the reef flat to

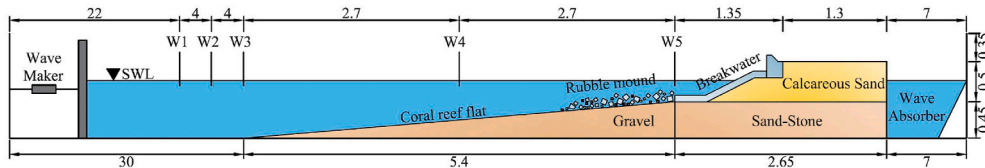


Fig. 1. Schematic map of the wave flume physical model (Unit: m).

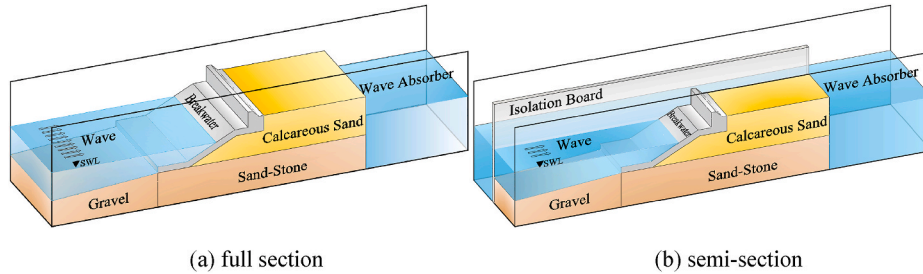


Fig. 2. Bird's-eye view of the wave flume physical model.

increase the surface roughness of the area. The sand-stones mixture is located directly beneath the calcareous sand foundation, with a length of 2.65 m and a height of 0.45 m. It is utilized to simulate the original stratum below the reclaimed land. The calcareous sand sampled from a reef island in the SCS is used to simulate the reclaimed reef island with a length of 2.25 m and a height of 0.5 m. The basic physical parameters of the calcareous sand are as follows: specific gravity $G_s = 2.83$ (Liu, 1999), coefficient of uniformity $C_U = 3.06$, coefficient of curvature $C_C = 1.15$, characteristic particle sizes are $d_{10} = 0.156$ mm, $d_{30} = 0.294$ mm, $d_{60} = 0.479$ mm, indicating that the in-situ calcareous sand is poorly graded and the particle size is mainly concentrated in the range of 0.1–0.5 mm. The particles gradation of the calcareous sand used in tests is demonstrated in Fig. 3.

A large amount of dry density measurement has been conducted by us in the field of reclaimed reef islands in the SCS. It is shown that the maximum dry density is $\rho_{dmax} = 1.54\text{g/cm}^3$ and the minimum dry density $\rho_{dmin} = 1.25\text{g/cm}^3$. The dry density of the calcareous sand

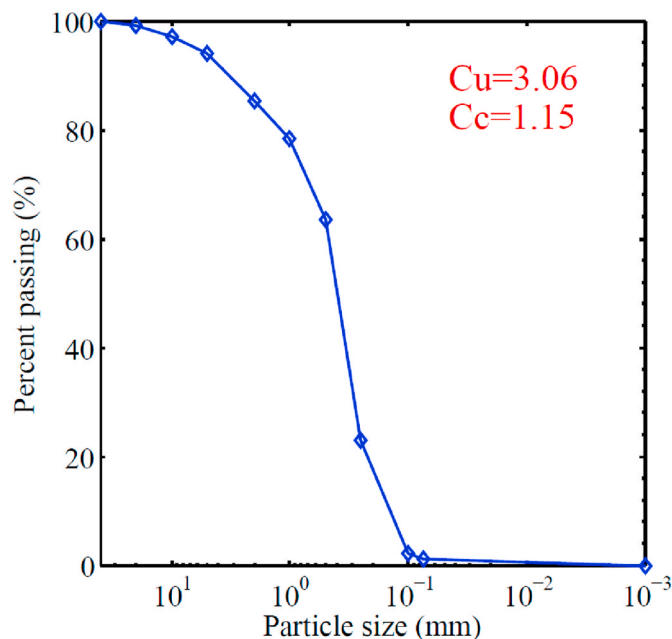


Fig. 3. Particles size gradation of the calcareous coral sand used in the tests.

foundation in the physical model in the tests is set as $\rho_d = 1.50\text{g/cm}^3$, its relative density $D_r = 0.885$. It is shown that the calcareous sand foundation is being in the dense state in the tests.

In this study, the model geometric scale of 1:10 is relatively large, which can significantly reduce the scale effects to a certain extent. However, in such a large-scale physical model test, it is extremely difficult to apply the geometric scale for the granular foundation materials, because there may be billions of soil particles need to be screened and crushed artificially. In previously published literature, it was never reported that a geometric scale was applied for the granular foundation materials in physical modelling tests in the field of offshore geotechnics. Such a practice could be only feasible in theory, but difficult to operate in practice. As a consequence, the particles sizes of the coral sand foundation are also not scaled in this study.

A series of measurement sensors are installed along the central longitudinal section of the flume. Among them, five wave profile gauges are installed along the center line of the flume to record the variation of water level during testing. The installment positions of the five wave profile gauges are listed in Table 2. Thirty pressure sensors are installed uniformly on the surface of the revetment breakwater to measure the wave impact pressure. However, only the pressure recorded by six sensors at typical positions as demonstrated in Fig. 4 are taken as the representatives for the analysis in this study. Two LVDT displacement sensors are installed on the left lateral side of the caisson wall to measure the horizontal and vertical displacement of the caisson. In the foundation of the physical model, totally sixteen pore pressure sensors are installed to record the pore pressure at typical positions. The layout of these measurement sensors is demonstrated in Fig. 4.

2.3. Wave condition

Based on the irregular characteristics of real ocean waves, random waves that are closer to the real ocean waves are generated in testing. JONSWAP spectrum is taken as the target spectrum for the generation of random waves in this study. The specific mathematical expression of JONSWAP spectrum is formulated by Equations (1)–(4) (Goda, 2000):

Table 2
Positions of the wave profile gauges (The left side of the flume is taken as the reference point).

No.	W1	W2	W3	W4	W5
Distance (m)	22.0	26.0	30.0	32.7	35.4

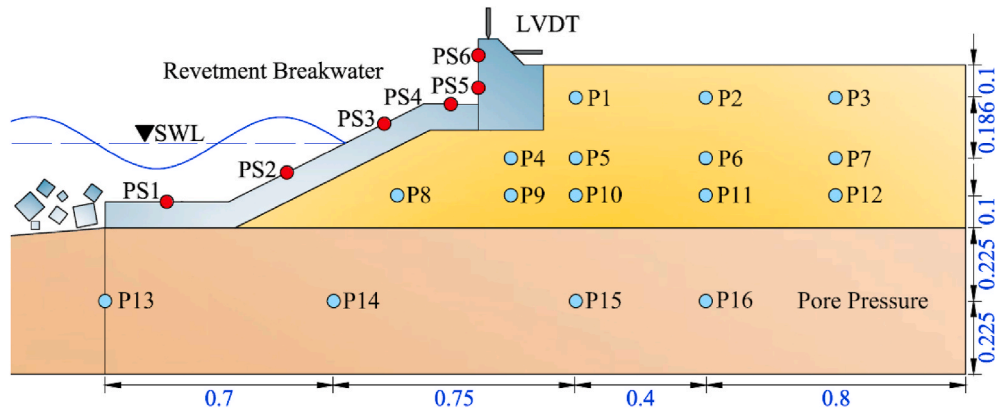


Fig. 4. Layout of measurement sensors in the physical model tests (Unit: m).

Table 3
Experimental conditions in the wave flume physical model tests.

Test No.	Water Depth (m)	Height (m)	Period (s)	Accropodes	Section
1	0.48	0.18	3.0	No	Semi-Section
2	0.48	0.23	1.7	No	Semi-Section
3	0.71	0.30	2.0	Yes	Full Section
4	0.71	0.30	2.0	No	Semi-Section
5	0.71	0.30	2.2	No	Semi-Section

$$S(f) = \beta_J H_s^2 T_p^{-4} f^{-5} \exp[-1.25(T_p f)^{-4}] \cdot \gamma^{\exp[-(f/f_p - 1)^2 / 2\sigma^2]} \quad (1)$$

in which

$$\beta_J = \frac{0.0624}{0.230 + 0.0336\gamma - 0.185(1.9 + \gamma)^{-1}} (1.094 - 0.01915 \ln \gamma) \quad (2)$$

$$T_p = \frac{T_s}{1 - 0.132(\gamma + 0.2)^{-0.559}} \quad (3)$$

$$\sigma = \begin{cases} 0.07 f \leq f_p \\ 0.09 f > f_p \end{cases} \quad (4)$$

where, $\gamma = 1 \sim 7$ (mean value is recommended as 3.3) is the peak enhancement factor governing the peak sharpness of JONSWAP spectrum, T_p is the peak period, f_p is the corresponding peak frequency, H_s is the effective wave height, T_s is the effective period.

In the design of the revetment breakwater, the fortified extreme ocean waves are 7 m high with a period of 10.0s in the deep sea around these coral reefs. CFD computation considering the real terrain of these coral reefs indicates that the fortified extreme ocean waves must break significantly due to the fact that the water depth suddenly reduces to a value less than 4 m on the reef flat once the deep-sea waves arriving at the reef flat of coral reefs. As a result, the effective wave height is only 3 m at the margin of the reef flat of coral reefs. Therefore, it is confirmed that the effective wave height of the random waves is 0.3 m or less based on the similarity ratio of 1:10. At the meantime, the effective period of



Fig. 5. A real view of the accropodes in front of the revetment breakwater.

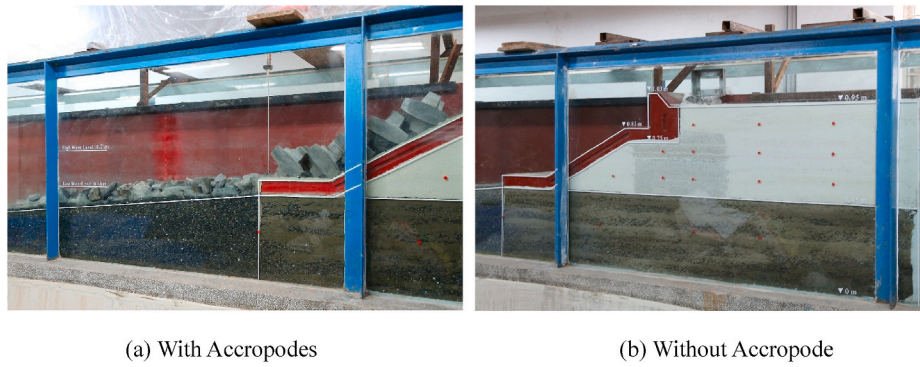


Fig. 6. A real view of the completed physical model with accropodes and without accropode.

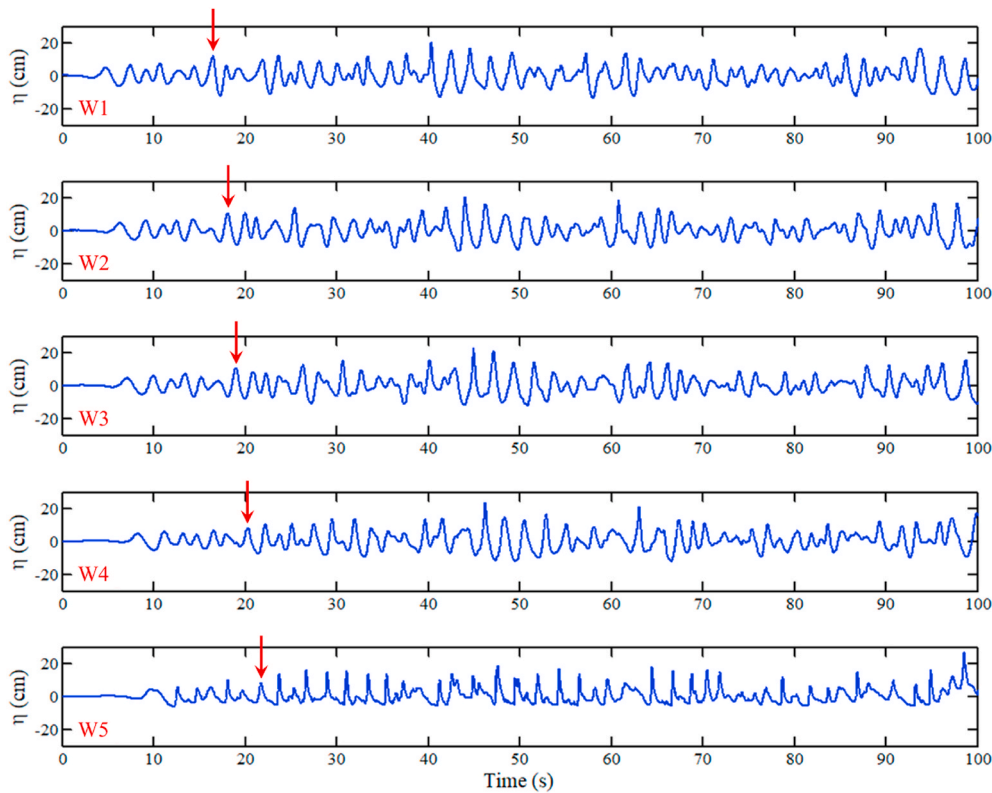


Fig. 7. Time history of the wave profiles measured by wave gauges in Test 3.

the random waves is set as 3.0 s or less according to the actual capability of the wave maker used in the flume. According to the field measurement of tides, the elevation difference between the extreme highest water level and the top of the caisson wall is around 3.46 m, and the elevation difference between the extreme lowest water level and the top of the caisson wall is about 5.52 m. Combined with the depth of the flume and the size of the physical model, it is determined that the water depth corresponding to the extreme highest water level and lowest water level is 0.71 m and 0.48 m, respectively by applying geometric similarity rule.

In this study, totally five test conditions listed in Table 3 are set for the wave flume tests. The time for the wave impacting the breakwater is 1–2 h in each test. During the Test 3, some accropodes are laid in front of the breakwater to dissipate wave energy, as depicted in Fig. 5. The calcareous sand foundation of the revetment breakwater is vibrated by a plate vibrator to the expected dry density layer by layer in the process of model preparation. Sensors are installed at designed locations as shown in Fig. 4. Fresh water is pumped into the flume reaching the specified

level, and then it is kept for 24 h for purpose of foundation saturation. Fig. 6 (a) and (b) illustrate the completed physical model under the condition with accropodes and without accropode, respectively.

3. Results and discussion

3.1. Validation of the generated JONSWAP waves

During the test, the wave profiles are collected by these installed gauges at the five typical positions. In order to verify the validity of the random waves generated by the wave maker, the spectrum analysis is performed for each test. Fig. 7 shows the time-history (0–100s) of the wave profiles recorded by the five wave gauges in Test 3. It can be seen that the wave profiles from W1 to W4 have obvious phase differences, and the wave profile measured by W5 has a significant attenuation.

The spectrum analysis for the time history of the wave profile recorded by W1 in the five tests is performed by FFT method. The comparison between the spectrum of these recorded wave profiles and

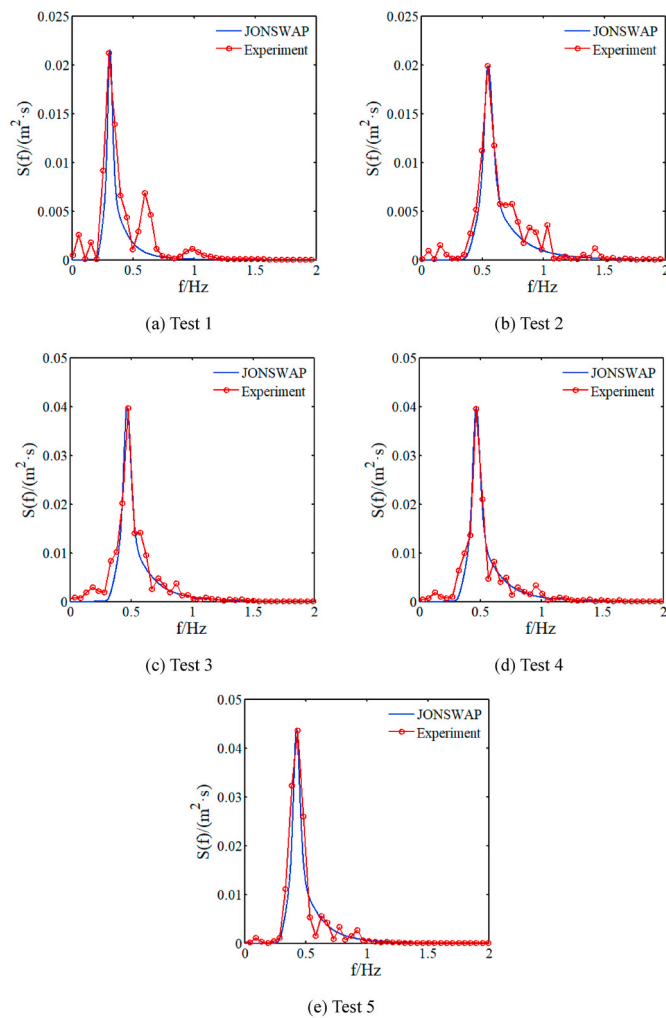


Fig. 8. Comparison between the test spectrum and the theoretical JONSWAP spectrum.

the theoretical spectrum of JONSWAP are illustrated in Fig. 8. It can be seen that the test spectrum and the target spectrum are in good agreement on the spectral shape, peak frequency and peak value. It is

indicated that the random waves with JONSWAP spectrum have been successfully generated in the five physical model tests.

3.2. Wave impact

It is well known that wave impact is the main external factor for the instability of breakwater. It is necessary to study it quantitatively. Fig. 9 illustrates the local time history of the wave impact recorded in Test 4 (hydrostatic pressure is excluded). It can be found that the wave impact on the breakwater is irregular. During the test, the wave impact recorded by PS1 is much disordered. It is attributed to the fact that PS1 is installed at the left flat section of the revetment breakwater, where the incident waves and reflected waves intensively interact, and the terrain near to there is complex. PS2 and PS3 are installed on the upper surface of the S-shaped revetment. The wave impact on PS2 fluctuates within the range of ± 1 kPa in most time, and it can reach 2 kPa at some moments under the attack of waves. The peak wave impact on PS3 is in the range of 0.7–1.2 kPa, and it can reach 3 kPa at some times.

PS4 is installed on the right end of the flat section of the S-shaped revetment. The peak wave impact on PS4 is slightly greater than that on PS3. PS5 and PS6 are installed on the left lateral side of the caisson wall, facing the incident waves directly. It can be observed that the peak wave impact at the two positions is greater than that on other positions. The peak wave impact on PS5 fluctuates in the range of 1.5–2.5 kPa at most times and it can reach maximally 5–6 kPa at some moments. It is also found in the test that the wave crests climb along the slope of revetment, collide with the caisson wall, then break and overtop once reaching the caisson wall. As a result, the wave impact on the side of the caisson wall is generally great. According to the geometric scale of 1:10, the maximum wave impact of the random waves on the caisson wall can be up to 50–60 kPa, and 20–30 kPa on the revetment. If taking into consideration of the test errors, the differences of terrain between the physical model and the in-situ situation, as well as giving a sufficient engineering safety redundancy, it is suggested that the peak wave impact on the caisson wall and on the revetment can be set as 100–120 kPa and 40–60 kPa, respectively in the design of the revetment breakwater.

Through the comparative analysis of the wave impact on the caisson wall for the five tests, it is found that the peak wave impact in the case with high water level is considerably higher than the case with low water level, and the peak wave impact in the case with accropodes is less than the case without accropode. Fig. 10 demonstrates the comparison of the wave impact on PS5 in Test 3 (with accropodes) and Test 4

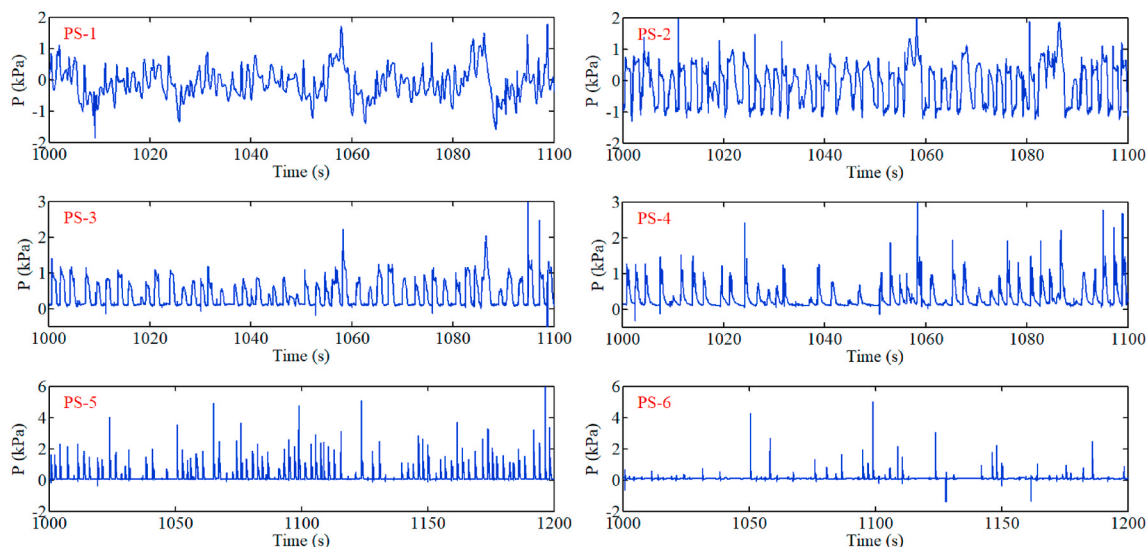
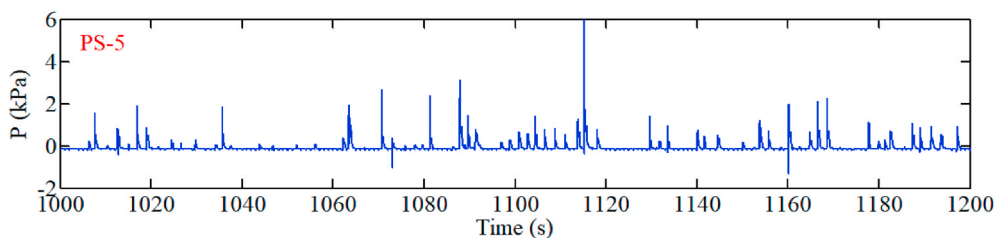
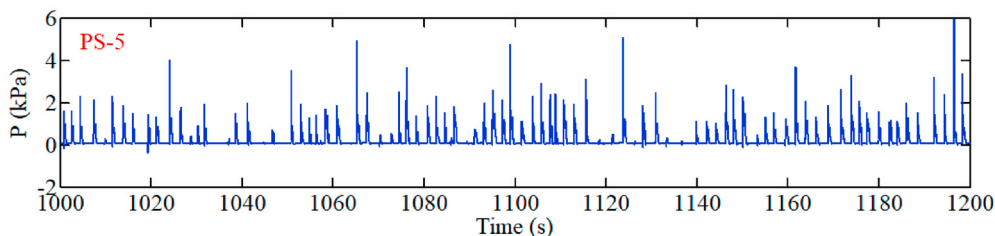


Fig. 9. Time history of the wave impact on the revetment breakwater in a typical time period measured in Test 4 (hydrostatic pressure is excluded).

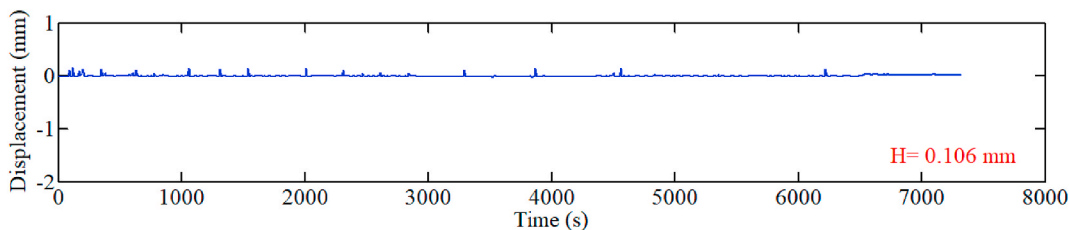


(a) Test 3

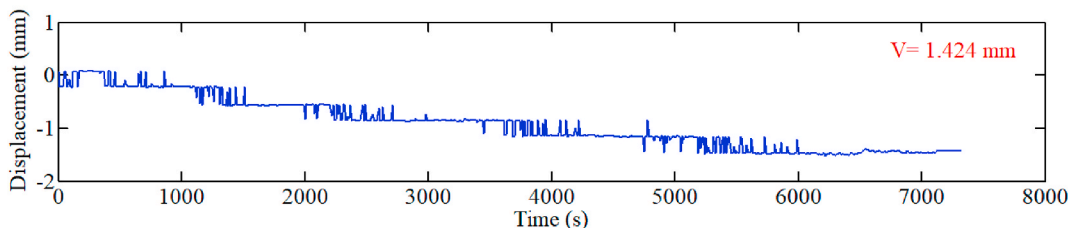


(b) Test 4

Fig. 10. Comparison of the wave impact on PS5 between Test 3 and Test 4.



(a) Horizontal displacement



(b) Vertical displacement

Fig. 11. Time history of the residual displacement of the caisson wall recorded in Test 4.

Table 4

Residual displacements of the caisson wall recorded in tests.

Test No.	1	2	3	4	5
H (mm)	0.025	0.049	0.063	0.106	0.124
V (mm)	0.030	0.077	0.034	1.424	0.271

(without accropode). It can be observed that the wave impact on the caisson wall is significantly reduced by the accropodes at most times. The peak wave impact remains below 1 kPa or even less at most times in Test 3. This result indicates that the wave energy absorption effect of the accropodes is very significant.

3.3. Displacement of the caisson wall

Fig. 11 shows the time history of the displacement of the caisson wall recorded in Test 4. It can be seen that the caisson wall moves very little

in horizontal direction. It only slightly fluctuates at some moments, and then returns to its initial position quickly under the continuous impacting by the waves. Eventually, the horizontal displacement is only 0.106 mm. Meanwhile, it is observed that the settlement of the caisson wall increases step by step. The vertical displacement is finally 1.424 mm after 2 h's wave impacting. It is indicated that the caisson wall mainly undergoes vertical settlement, and it can be considered that the breakwater is stable due to its minor displacement under the severe wave impact.

The residual displacements of the caisson wall recorded in the five tests are all listed in Table 4. It is found that there is no significant movement occurring for the caisson wall in the five tests. The structural displacement recorded in Test 3 (with accropodes) indicates that accropodes can effectively reduce the displacement of the caisson wall. It is also confirmed that the energy absorption effect of the accropodes is obvious. There is no evident deformation and destruction observed in the dense calcareous sand foundation in the five tests. From the

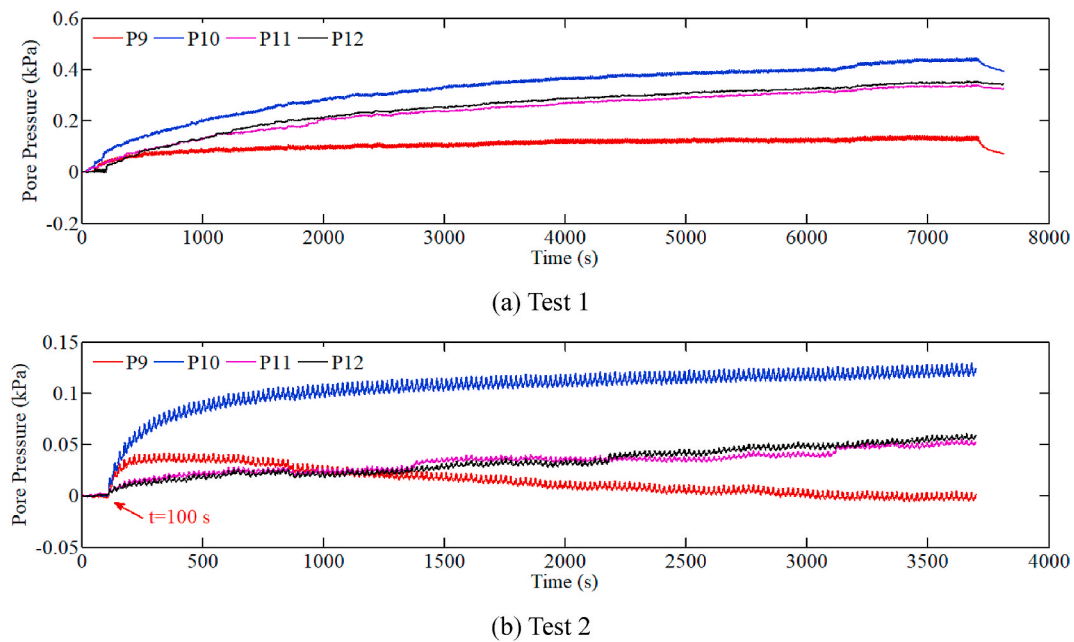


Fig. 12. Time history of the pore pressure in the calcareous sand foundation recorded by P9 to P12 in Test 1 and Test 2.

perspective of displacement of structure and deformation in the foundation, it is confirmed that the revetment breakwater can remain stable state under the long-time impact of waves.

3.4. Characteristics of pore pressure accumulation

The accumulation of pore pressure in sand foundation is mainly caused by two mechanism: (1) The increase of the water level inside the calcareous sand foundation caused by the continuous wave overtopping; (2) Plastic volumetric deformation occurs in the foundation under the continuous impacting of waves, which could result in the build-up of pore pressure. Excessive development of pore pressure would result in the residual liquefaction or stiffness softening occurring in the calcareous sand foundation. Generally, the second mechanism related to the residual pore pressure would be the main cause of breakwater instability (Wang et al., 2015). Generally, residual liquefaction frequently occurs in loose fine sand, but it can also occur in dense sand. Whether the liquefaction occurring depends on the strength and frequency of external dynamic loading, as well as the drainage performance of foundation soil and the length of drainage path inside foundation. It is not only determined by the single factor of the type of foundation soil. In this study, there is also the accumulation of pore pressure observed in the dense foundation. Therefore, it is necessary to explore whether the liquefaction occurs or not in the coral sand foundation under wave impact.

In order to explore the development characteristics of pore pressure in the dense calcareous sand foundation in the five tests, the results of pore pressure recorded in Test 1 and Test 2 in which low water level is involved are firstly analyzed. Fig. 12 shows the time history of the pore pressure recorded by P9 to P12 in Test 1 and Test 2. It can be found that the pore pressure increases with different magnitudes during testing. According to the observation by bare eyes, there is no water overtopping occurring in Test 1 and Test 2 due to the low water level. Therefore, the accumulation of pore pressure is definitely not caused by the wave overtopping. As a result, it can be confirmed that the accumulation of pore pressure in the foundation in the cases with low water level is only due to the occurrence of plastic volumetric strain in the calcareous sand foundation. Under the cyclic impact of the random waves, the pore pressure in the foundation gradually increases, and then dissipates after the wave stopping to impact. It is also observed that the magnitude of the accumulated pore pressure in the calcareous sand foundation are all

not significant in Test 1 and Test 2, only in the range of 0–0.5 kPa. This magnitude of residual pore pressure is generally impossible to make the calcareous sand become liquefied. The phenomenon of non-liquefaction of the calcareous sand foundation is beneficial for the revetment breakwater to stay stable under the severe impact of ocean waves.

Secondly, based on the observation for the overtopping, it is found that wave overtopping occurs in the Test 3, 4 and 5 in which high water level is involved. Therefore, the accumulation of pore pressure under high water level condition is the combined result of the overtopping of random waves, as well as the plastic volumetric strain in the calcareous sand foundation. Fig. 13 demonstrates the time history of the pore pressure recorded in Test 3 (P.S. The pore pressure sensor P8 is broken and the data is missed). As observed in Fig. 13, there are some large-amplitude oscillation with a period of about 300s in the time history of pore pressure. This phenomenon would be attributed to the fact that the physical model in Test 3 is made along the full section of the wave flume. It leads to the result that the incident wave is completely blocked by the physical model. As a result, the energy of reflected waves cannot be dissipated effectively. With the gradual accumulation of the reflected wave energy in the wave flume, its effect on the incident wave and water level becomes more and more significant. Finally, the water level oscillation with a period of 300s is formed in the wave flume.

In Test 3, P1 to P3 are installed in the upper part of the calcareous sand foundation. The pore pressure could dissipate timely due to the proximity to the surface. Thus, the accumulation of pore pressure in the upper part of foundation is not significant, only in the range of 0–0.5 kPa. P4 to P7 are located in the middle part of the calcareous sand foundation. Among them, the pore pressure recorded by P4, P5 and P6 increases obviously, with a magnitude of about 0.8–1.1 kPa. It is only due to the fact that P7 is placed at the position near to the right lateral end of the model. The response of pore pressure on P7 is relatively weak with a magnitude of 0.1–0.2 kPa. P9 to P12 are allocated at the bottom of the calcareous sand foundation. The residual pore pressure is only about 0.3–0.6 kPa on P9 to P12, because P9 to P12 are adjacent to the sand-stones mixture layer which has a great permeability coefficient, making the pore pressure not to be accumulated easily. P13 to P16 are located in the sand-stone foundation, in which excess pore pressure can dissipate timely as a result of the excellent permeability. In addition, it is found that with getting closer to the reef flat, the amplitude of the oscillatory pore pressure becomes greater, e.g., the pore pressure

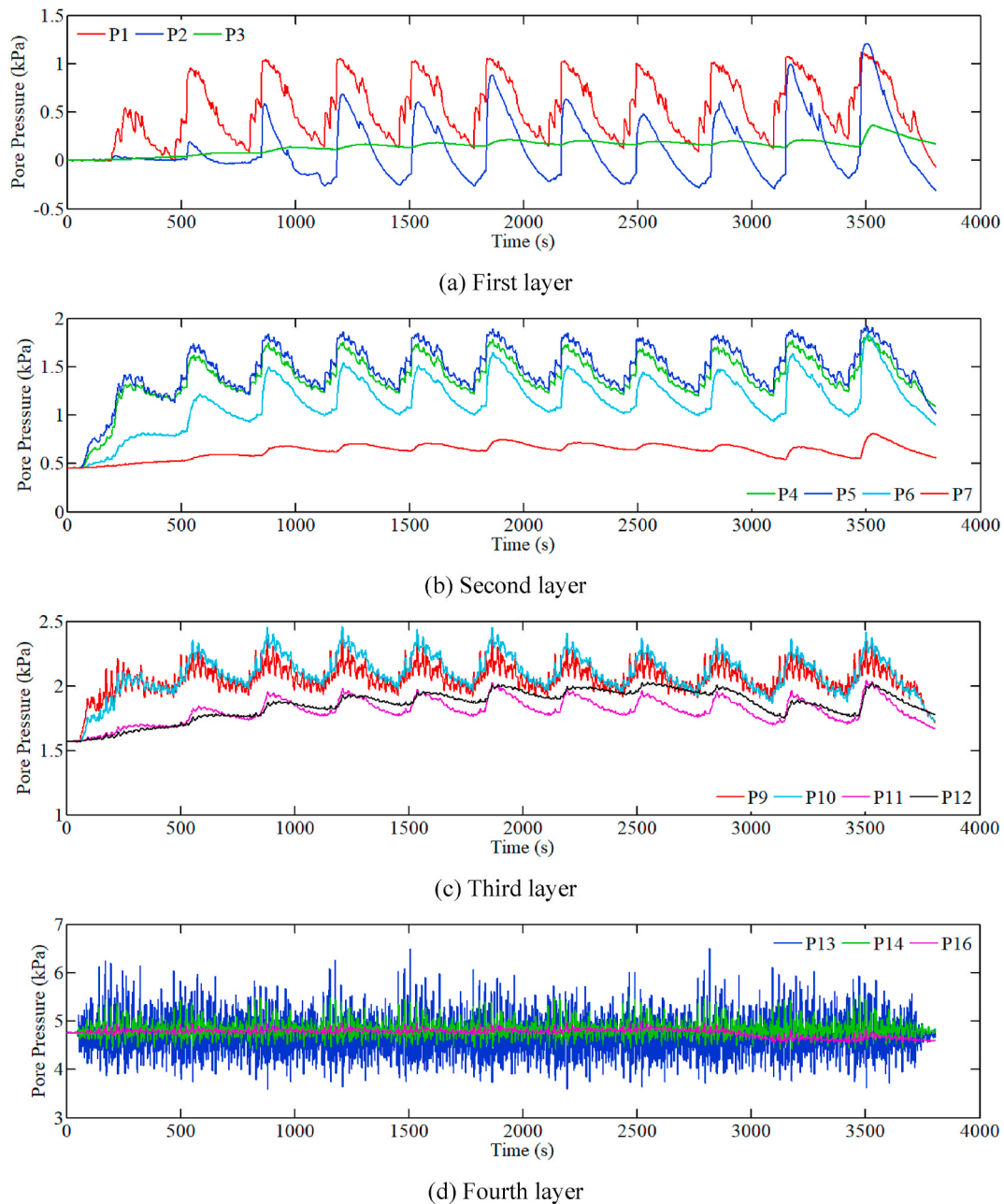


Fig. 13. Time history of the pore pressure in the calcareous sand foundation in Test 3 (with accropodes).

recorded by P13.

Fig. 14 illustrates the time history of the pore pressure recorded in Test 4 without accropode (P.S. P8 is broken and its data is missing). It can be seen that the amplitude of oscillation in the time history of the pore pressure reduces significantly, which might be due to the fact that the physical model is made along the semi-section of the wave flume in Test 4. Most of the energy of reflected waves can be dissipated in the wave absorption section. As a result, the effect of the reflected wave energy on the incident wave and water level is quite small. Based on this test result, it can be found that the semi-section of the physical model has an obvious advantage for this study.

As shown in Fig. 14, the accumulation of pore pressure recorded by P1 to P3 has little difference with a magnitude of 1.3–1.5 kPa. However, the responses of the pore pressure recorded by the sensors buried in the second and third layer are quite different, which shows that the maximum residual pore pressure in the second-layer is 2.5 kPa, while the value is approximately 1.5 kPa in the third-layer. The accumulation

of pore pressure recorded in Test 4 (without accropode) are much greater than that in Test 3 (with accropodes). It is indicated that accropodes can significantly weaken the wave impact and reduce the accumulation of pore pressure in the calcareous sand foundation. Therefore, accropodes are very beneficial to the stability of breakwater.

In this study, the initial stress at the position of P1 to P12 cannot be directly measured, and the accumulation of the pore pressure caused by the overtopping of random waves and the plastic volumetric strain in the calcareous sand foundation can't be separated. Therefore, it is difficult to directly determine whether the foundation is liquefied based on the accumulated magnitude of pore pressure. However, further analysis of the time history of the displacement of the caisson wall in the five tests indicates that there is no liquefaction occurring in the dense calcareous sand foundation, because the displacement of the caisson wall is quite minor. Otherwise, the caisson wall will have a great displacement and the whole physical model would lose its stability.

It should be noted that the permeability of the coral sand foundation

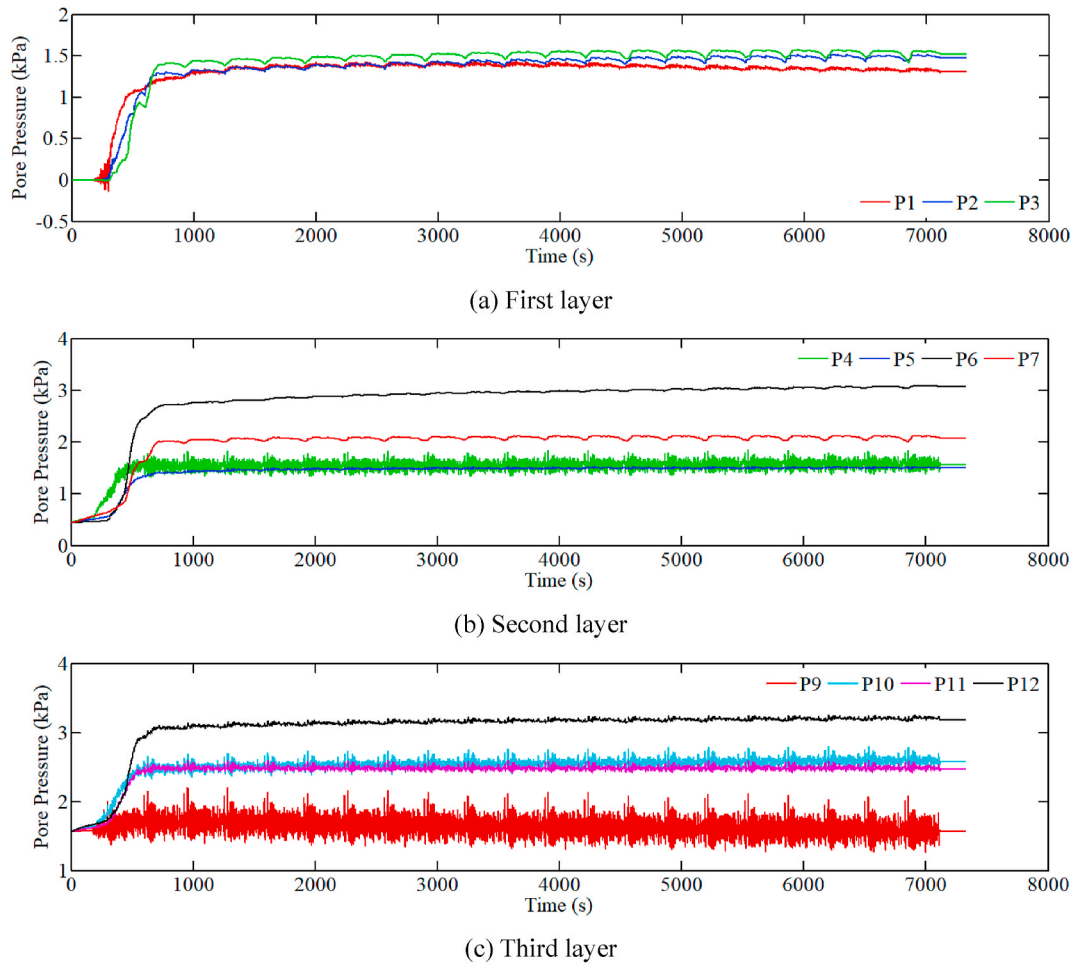


Fig. 14. Time history of the pore pressure recorded in Test 4 (without accropode).



Fig. 15. A real view of the wave impacting and the water overtopping at a moment.

in the physical model must have been slightly amplified compared with that in prototype foundation due to the fact that the model geometric scale of 1:10 has not been applied to the granular foundation materials. As a result, the magnitude of pore pressure accumulation would be underestimated in the tests relative to that in prototype foundation. Therefore, the analysis on the accumulation of pore pressure and the residual liquefaction in the coral sand foundation presented here need to be understood adopting a dialectical way.

3.5. Wave overtopping

During the tests, a device is used to collect the water that crosses the breakwater. The amount of wave overtopping is recorded every 2 min in

testing. In Test 1 and Test 2, there is no water overtopping observed when the water level is low. However, significant water overtopping is observed in Test 3, 4 and 5, as shown in Fig. 15. Fig. 16 illustrates the time history of the accumulated water volume of the random waves overtopping measured in Test 3, 4 and 5. In Fig. 16 (a), it is found that the usage of accropodes can effectively reduce the amount of wave overtopping from 0.39 m³/h to 0.10 m³/h per meter, reducing about 74.4%. In practical engineering, the usage of accropodes could be an encouraged way to reduce the water overtopping.

Fig. 16 (b) demonstrates the comparison of the overtopping between Test 4 (T_S = 2.0s) and Test 5 (T_S = 2.2s). It can be found that the amount of wave overtopping is basically the same while the effective period increases from 2.0s to 2.2s. It is indicated that the wave period has a

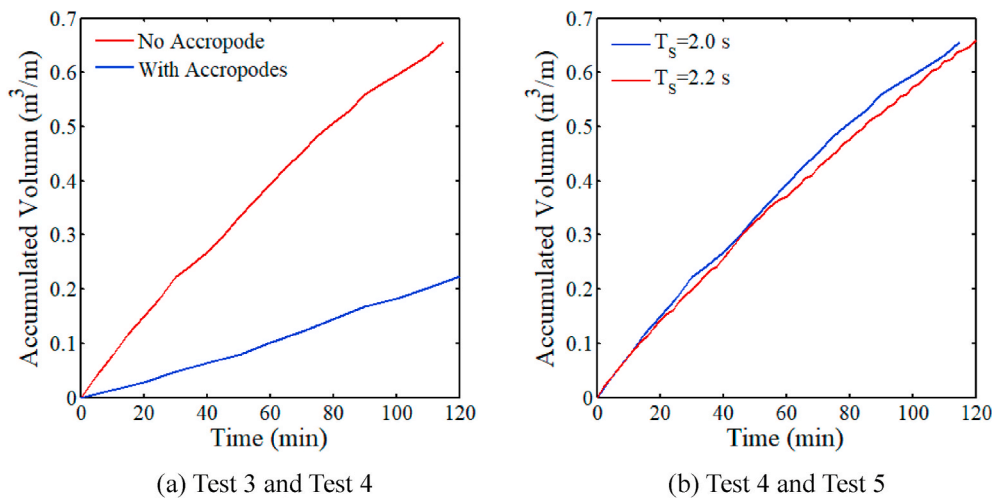


Fig. 16. Comparison of the accumulated volume of wave overtopping in Test 3, 4 and 5.

minor effect on the overtopping. According to the similarity ratio of volume 1:100, as listed in Table 1, it can be inferred that the volume of wave overtopping over the revetment breakwaters built on the reclaimed reef islands can reach 39ton/h per meter without installing accropodes in front of the breakwater. Once a large amount of water crosses over the breakwater, only little could be discharged through the drainage facilities. As a consequence, most of the overtopped water will seep into the calcareous sand foundation. It definitely will adversely affect the formation process of the underground desalted water in these reclaimed coral reef islands. Finally, it is known from the wave flume physical model tests that the usage of accropodes in front of the revetment breakwater and the enhanced drainage capacity can be very beneficial to protect the underground desalted water in the reclaimed calcareous sand foundation.

4. Conclusion

In this study, taking the reclamation project of the coral reef islands in the SCS as the background, the dynamics and stability of the revetment breakwater and its dense calcareous sand foundation are investigated by performing a series of wave flume physical model tests considering different wave conditions for the first time in the field of offshore geotechnics. This work could provide ocean engineers with an insightful understanding on the dynamics characteristics, and on the possible instability modes of the revetment breakwater and its coral sand foundation under the impact of extreme ocean waves, which will be beneficial for the design and maintenance of the revetment breakwater in the SCS in the future. Through comprehensive analysis, the following conclusions are obtained:

- (1) The random waves generated by the wave maker are effective and basically agreeable with the theoretical JONSWAP spectrum. Under the attack of fortified random waves, the maximum wave impact on the revetment and the caisson wall are 2–3 kPa and 5–6 kPa, respectively. According to the model geometric scale 1:10, the impact pressure of the fortified waves on the revetment and the caisson wall in practical engineering could reach 20–30 kPa and 50–60 kPa, respectively. Considering the terrain difference between the physical model and the in-situ situation, as well as reserving sufficient engineering safety redundancy, it is suggested that the wave impact for design on the revetment and on the caisson wall can be selected as 40–60 kPa and 100–120 kPa, respectively.
- (2) Under the continuous impacting of waves, there is no significant displacement occurring for the breakwater. The maximum

horizontal displacement and vertical settlement are only 0.124 mm and 1.424 mm in the five tests. Furthermore, it is observed that there is also no significant deformation occurring in the calcareous sand foundation. Overall, the revetment breakwater built on the dense calcareous sand foundation can keep stable under the attack of fortified ocean wave.

- (3) In the five tests, the accumulation of pore pressure in the calcareous sand foundation is generally small. The maximum residual pore pressure can reach 3 kPa. There is a significant oscillation in the time history of the pore pressure in the dense calcareous sand foundation if the physical model is made along the full section of flume. However, this oscillation could basically disappear if the physical model is made in the way of semi-section. Accropodes can effectively weaken the response of pore pressure.
- (4) There is no wave overtopping crossing the breakwater under the condition of low water level. The wave overtopping under high water level condition needs to be considered in practical engineering. Under the condition without accropode, the volume of wave overtopping can reach 0.39 m³/h per meter. By the usage of accropodes in front of the revetment breakwater, wave overtopping could reduce by about 74.4%. According to the conversion relation adopting the similarity ratio, the wave overtopping crossing the prototype revetment breakwater in the SCS could reach 39 ton/h per meter. This wave overtopping will definitely have a fatal influence on the ecological environment of the reclaimed reef islands.
- (5) Accropodes can play a critical role in wave energy dissipation. They can weaken the wave impact on the breakwater and effectively reduce the displacement of the caisson wall and the amount of wave overtopping. The reasonable usage of accropodes in practical engineering can significantly improve the overall stability of the revetment breakwater built on the reclaimed coral reef islands in the SCS.

CRediT authorship contribution statement

Yu Zhang: Investigation, Visualization, Formal analysis, Writing - original draft. **Jianhong Ye:** Conceptualization, Methodology, Writing, Supervision, Project administration, Funding acquisition.

Declaration of competing interest

The authors declare that they have no known competing financial interests or personal relationships that could have appeared to influence

the work reported in this paper.

Acknowledgement

This work is grateful for the funding support from “Strategic Priority Research Program of the Chinese Academy of Sciences”, Grant No. XDA13010202, as well as the funding support from National Natural Science Foundation of China, Grant No. 51879257.

References

- Aminti, P., Franco, L., 1988. Wave overtopping on rubble mound breakwaters. *Coast Eng.* 1989, 770–781. <https://doi.org/10.1061/9780872626874.058>.
- She-an, Bie, Zhao, Zi-dan, Liu, Tong-li, et al., 1997. Model test of wave-induced pore pressure in the sandy seabed. *Mar. Sci. Bull.* 55–65, 05.
- Biot, M.A., 1941. General theory of three-dimensional consolidation. *J. Appl. Phys.* 12 (2), 155–164. <https://doi.org/10.1063/1.1712886>.
- Chen, Songgui, Chen, Hanbao, Zhao, Hongbo, et al., 2019. Experimental study of wave forces on the seawall of coral reef in large wave flume. *Journal of Hohai University (Natural Sciences)* 47, 65–70. <https://doi.org/10.3876/j.issn.1000-1980.2019.01.010>, 01.
- Demars, K.R., Vanover, E.A., 1985. Measurement of wave-induced pressures and stresses in a sandbed. *Mar. Geosour. Geotechnol.* 6 (1), 29–59. <https://doi.org/10.1080/10641198509388179>.
- Galland, J.C., 1994. Rubble mound breakwater stability under oblique waves: an experimental study. *Coast Eng.* 1995, 1061–1074. <https://doi.org/10.1061/9780784400890.078>.
- Gatmiri, B., 1990. A simplified finite element analysis of wave-induced effective stresses and pore pressures in permeable sea beds. *Geotechnique* 40 (1), 15–30. <https://doi.org/10.1680/geot.1990.40.1.15>.
- Goda, Y., 2000. *Random Seas and Design of Marine Structures*. World Scientific Press, Singapore.
- Hsu, J.R.C., Jeng, D.S., 1994. Wave-induced soil response in an unsaturated anisotropic seabed of finite thickness. *Int. J. Numer. Anal. Methods GeoMech.* 18 (11), 785–807. <https://doi.org/10.1002/nag.1610181104>.
- Jeng, D.S., Cha, D.H., Lin, Y.S., et al., 2001. Wave-induced pore pressure around a composite breakwater. *Ocean Eng.* 28 (10), 1413–1435. [https://doi.org/10.1016/S0029-8018\(00\)00059-7](https://doi.org/10.1016/S0029-8018(00)00059-7).
- Ju, L.H., 2004. *Physical Model Test and Analysis of Wave Force and Overtopping of Typical Breast Wall*. PhD Thesis. Nanjing Hydraulic Research Institute, China.
- Kirca, V.S.O., Sumer, B.M., Fredsøe, J., 2013. Residual liquefaction of seabed under standing waves. *J. Waterw. Port, Coast. Ocean Eng.* 139 (6), 489–501. [https://doi.org/10.1061/\(ASCE\)WW.1943-5460.0000208](https://doi.org/10.1061/(ASCE)WW.1943-5460.0000208).
- Chong-quan, Liu, 1999. *The Theory of Calcareous Soils Mechanics and its Application in Engineering*. PhD thesis. Institute of Rock and Soil Mechanics, Chinese Academy of Sciences.
- Lu, Hai-bin, 2005. *The Research on Pore Water Pressure Response to Waves in Sandy Seabed*. PhD thesis. Changsha University of Science & Technology, China.
- Madsen, O.S., 1978. Wave-induced pore pressures and effective stresses in a porous bed. *Geotechnique* 28 (4), 377–393. <https://doi.org/10.1680/geot.1978.28.4.377>.
- Mizutani, N., Mostafa, A.M., Iwata, K., 1998. Nonlinear regular wave, submerged breakwater and seabed dynamic interaction. *Coast Eng.* 33 (2–3), 177–202. [https://doi.org/10.1016/S0378-3839\(98\)00008-8](https://doi.org/10.1016/S0378-3839(98)00008-8).
- Mostafa, A.M., Mizutani, N., Iwata, K., 1999. Nonlinear wave, composite breakwater, and seabed dynamic interaction. *J. Waterw. Port, Coast. Ocean Eng.* 125 (2), 88–97. [https://doi.org/10.1061/\(ASCE\)0733-950X\(1999\)125:2\(88\)](https://doi.org/10.1061/(ASCE)0733-950X(1999)125:2(88)).
- Sumer, B.M., Hatipoglu, F., Fredsøe, J., Sumer, S.K., 2006. The sequence of sediment behavior during wave-induced liquefaction. *Sedimentology* 53 (3), 611–629. <https://doi.org/10.1111/j.1365-3091.2006.00763.x>.
- Tzang, S.Y., 1992. *Water Wave-Induced Soil Fluidization in a Cohesionless Fine-Grained Seabed*. PhD these. University of California, Berkeley, USA.
- Wang, Li-zhong, Dong-zi, Pan, Pan, Cun-hong, Hu, J., 2007. Experimental investigation on wave-induced response of seabed. *China Civ. Eng. J.* 40, 101–109. <https://doi.org/10.15951/j.tmgxcb.2007.09.016>.
- Wang, Liang-min, Ye, J.H., Chang-qi, Zhu, 2015. Investigation on the wave-induced progressive liquefaction of offshore loosely deposited sandy seabed. *Rock Soil Mech.* 36 (12), 3583–3588. <https://doi.org/10.16285/j.rsm.2015.12.031>.
- Yamamoto, T., Koning, H.L., Sellmeijer, H., et al., 1978. On the response of a poro-elastic seabed to water waves. *J. Fluid Mech.* 87 (1), 193–206. <https://doi.org/10.1017/S0022112078003006>.
- Yamini, O.A., Kavianpour, M.R., Mousavi, S.H., 2017. Experimental investigation of parameters affecting the stability of articulated concrete block mattress under wave attack. *Appl. Ocean Res.* 64, 184–202. <https://doi.org/10.1016/j.apor.2017.03.003>.
- Yamini, O.A., Kavianpour, M.R., Mousavi, S.H., 2018. Wave run-up and rundown on ACB Mats under granular and geotextile filters' condition. *Mar. Geosour. Geotechnol.* 36 (8), 895–906. <https://doi.org/10.1080/1064119X.2017.1397068>.
- Yan, Z., Zhang, H.Q., Sun, X.P., 2018. Tests on wave-induced dynamic response and instability of silty clay seabeds around a semi-circular breakwater. *Appl. Ocean Res.* 78, 1–13. <https://doi.org/10.1016/j.apor.2018.05.014>.
- Ye, J.H., Wang, G., 2015. Seismic dynamics of offshore breakwater on liquefiable seabed foundation. *Soil Dynam. Earthq. Eng.* 76, 86–99. <https://doi.org/10.1016/j.soildyn.2015.02.003>.
- Ye, J.H., Jeng, D.S., Wang, R., Zhu, C.Q., 2013a. Validation of a 2D semi-coupled numerical model for fluid-structure-seabed interaction. *J. Fluid Struct.* 42, 333–357. <https://doi.org/10.1016/j.jfluidstructs.2013.04.008>.
- Ye, J.H., Jeng, D.S., Wang, R., Zhu, C.Q., 2013b. A 3D semi-coupled numerical model for fluid-structures-seabed-interaction (FSSI-CAS 3D): model and verification. *J. Fluid Struct.* 40, 148–162. <https://doi.org/10.1016/j.jfluidstructs.2013.03.017>.
- Ye, J.H., Jeng, D.S., Liu, P.L.F., Chan, A.H.C., Wang, R., Zhu, C.Q., 2014. Breaking wave-induced response of composite breakwater and liquefaction in seabed foundation. *Coast Eng.* 85, 72–86. <https://doi.org/10.1016/j.coastaleng.2013.08.003>.
- Ye, J.H., He, K.P., Shan, J.P., 2019. Experimental study on stability of revetment breakwater built on reclaimed coral reef islands in South China Sea under extreme wave impact. *Blasting* 36 (4), 13–23. <https://doi.org/10.3963/j.issn.1001-487X.2019.04.002>.
- Zen, K., Yamazaki, H., 1990. Mechanism of wave-induced liquefaction and densification in seabed. *Soils Found.* 30 (4), 90–104. <https://doi.org/10.3208/sandf1972.30.4.90>.
- Zhang, F., Ge, Z., 1996. A study on some causes of rubble mound breakwater failure. *China Ocean Eng.* 10 (4), 473–481.